ARTICLE IN PRESS

Available online at www.sciencedirect.com
SCIENCE DIRECT®

Journal of Process Control xxx (2005) xxx–xxx

JOURNAL OF PROCESS CONTROL

www.elsevier.com/locate/jprocont

A hybrid nonlinear state observer for concentration profiles reconstruction in nonlinear simulated moving bed

J.P. Corriou [a], M. Alamir [b,*]

[a] Laboratoire des Sciences du Génie-Chimique, Groupe ENSIC, 1, rue Grandville, BP. 451, 54001 Nancy Cedex, France
[b] Laboratoire d'Automatique de Grenoble, CNRS/INPG/UJF, LAG/ENSIEG UMR 5528, BP 46, Domaine Universitaire, 38400 Saint Martin d'Hères, France

Received 21 July 2004; received in revised form 20 June 2005; accepted 4 July 2005

Abstract

In this paper, a state observer is proposed for the reconstruction of the concentration profiles in a simulated moving bed. The approach is based on a simple Luenberger-like correction term. The observer is used under the assumption that the flow rates are constant during each switching period. The matrix gain of the correction term may then be re-computed at the beginning of each switching period corresponding to flow rates being changed by the controller. Validating simulations are proposed to assess the efficiency of the proposed profile reconstruction and its robustness against uncertainties on modelling parameters. Comparisons are also done with open-loop simulation based-observer in order to strengthen the relevance of the correction term.

Keywords: Nonlinear observer; SMB; State estimation; Concentration profiles reconstruction

1. Introduction

In industrial domains such as food, fine chemicals and pharmaceutical production where high purities and yields are required, chromatographic separations are commonly used. To avoid the drawbacks of batch chromatography, the continuous true moving bed (TMB) has been conceived where the solid and liquid phases move in a countercurrent way. However, in the latter process, the solid adsorbent would be rapidly deteriorated due to attrition of adsorbent particles, so that it is preferable to simulate its movement in a continuous countercurrent chromatographic process, the simulated moving bed (SMB) (Fig. 1) by cyclic switching of the inlet and outlet ports corresponding to feed, eluent, extract and raffinate, in the direction of the fluid flow. A typical SMB is constituted of four sections, each of them being composed of two chromatographic columns. Consider a binary mixture (A,B) transported with the solvent in the feed between Sections 2 and 3. One component A is more adsorbable and B less adsorbable by the the adsorbent which forms the motionless solid phase. The separation occurs in the central Sections 2 and 3. Before the end of the switching time, B is driven upwards by the eluent (or desorbent) in the direction of the fluid flow (Section 3) while A is retained in this section. In Section 4, B is adsorbed in absence of A and withdrawn back in the raffinate while the eluent is regenerated. The more adsorbable component A remains adsorbed on the solid phase until it reaches Section 1. Section 1 is used to desorb A which is collected in the extract and the adsorbent is regenerated. A cyclic steady state occurs after many valve switches. Thus the continuous process of the SMB first patented by UOP [3] has been developed [27,6,25]. Main applications include the large scale separations of xylenes in the Eluxyl process

* Corresponding author. Tel.: +33 47 682 6326; fax: +33 47 682 6388.
E-mail address: mazen.alamir@inpg.fr (M. Alamir).

0959-1524/$ - see front matter © 2005 Elsevier Ltd. All rights reserved.
doi:10.1016/j.jprocont.2005.07.002

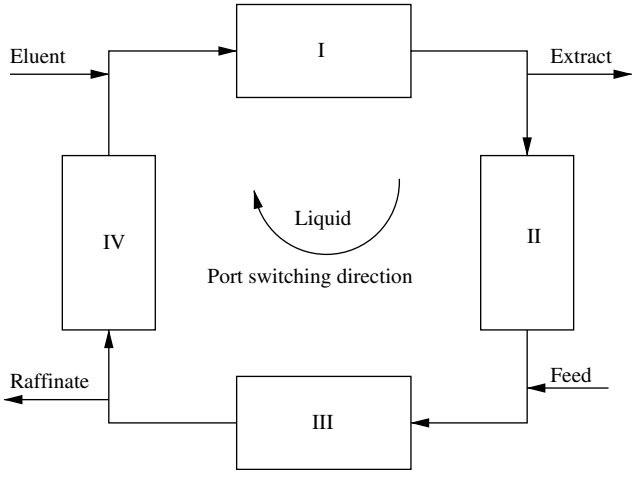

Fig. 1. Scheme of the simulated moving bed.

patented by IFP [8] and of fructose and glucose in the food industry [26,5]. Concerning high-value products, the separation of enantiomers of chiral drugs has drawn much attention in particular because of very high performances of the SMB and the economy on the solvent consumption [13,18,14].

The SMB has been studied in the literature concerning different aspects including modelling and simulation [10,11,9,30], design [28,4,22] with new concepts as the Varicol process [20], optimization for selection of optimal operating conditions and respect of operating constraints [23,8,19] and control using multivariable linear constrained control [8,12], model-based control [24,15], nonlinear geometric control [29,17]. More recently, a flexible nonlinear predictive control has been proposed [2] to handle auxiliary cost functions that may change during the production.

Papers concerning the design of observers for the SMB are less common though it is an important issue. This is due to the problems generally posed by distributed systems represented by partial differential equations, where high dimensional observability problems often occur.

For their observer development, [21] considered the case of the separation of xylenes for the process operated by the Institut Français du Pétrole. The nonlinear detailed model of fluid adsorption in a fixed bed contains four phases with the fluid in the interparticle space, the fluid in the macro and mesopores, the adsorbed phase in the micropores and the solid adsorbent. This model is stable but too complex. Consequently, they developed a state observer based on the linearized model. The observer is then improved by addition of estimation of the fluid flow velocity. The final observer for the SMB includes state correction with the correction gain being computed by heuristic approach based on physical considerations and simulation studies.

A very different observer is developed by [16]. Here, only the stationary regime which results in a periodic behaviour of the SMB is considered. The model includes convection and diffusion and the binary system is described by a linear isotherm. They assumed that measurements at the separations between the sections of the SMB are available only at switching instants and are provided by analytical chromatography. The objective of their observer is to determine the form, position and propagation velocity of the distributed concentrations $c_i(t,z)$. For that purpose, a dynamical model of the four wave fronts is derived as follows:

$$c_i(\tau,z,k) = \exp(b_i(z-(v_{c,i}\tau + z_{0,i}))) \quad (1)$$

where i is the wave front subscript, k the index for a switching period, τ any instant during a switching period, v_c the propagation velocity. This equation depends on three physical parameters which are constant over a given switching period. Then three state variables, based on the parameters, respectively, $x_1 = b(k)$, $x_2 = -b(k)v_c(k)$ and $x_3 = -b(k)z_0(k)$ are introduced to define a three-dimensional discrete state-space model which is the state equation of the wave model. To solve the observation problem, the measurement time is varied at each switching period.

In [1], a nonlinear receding horizon estimation scheme with adjustable precision is proposed. The scheme approximates the concentration profiles over a suitable truncated functional basis. The resulting vector of unknowns is first reduced using available measurements. The remaining part is then computed by nonlinear optimization. The scheme is conceptually very general. However, in order to achieve high precision estimation, high dimensional optimization problems have to be invoked that may be difficult to solve in real time.

In this paper, an estimation scheme is proposed that is dedicated to processes in which the main phenomena are linear and where nonlinearities are present but as second order terms (this is typically the case of many SMB processes with nonlinear isotherms). The use of high gain-like approach enables then to "*kill*" the bad effects of nonlinearities on the quality of the overall estimation. Furthermore, unlike the design approach proposed in [21] where the correction gain is computed heuristically, the approach proposed in this paper is based on the use of Riccati-like approach to systematically compute the correction gain.

The paper is organized as follows: the estimation scheme is first presented in Section 2 in a general context. The SMB equations are recalled in Section 3 and the way they can be put in the general form of Section 2 is detailed. Finally, illustrative simulation results are proposed in Section 4 in order to assess the efficiency of the proposed scheme in estimating the concentration profiles in the the columns despite significant errors in the system's parameters knowledge.

2. Theoretical background

In this section, the general theoretical background underlying the proposed state reconstruction scheme is presented. To this respect, the methodology used hereafter can be applied to a class of nonlinear systems that are issued from the transformation of partial differential equations into ordinary differential equations using discretization scheme (collocation, finite differences, series of ideal reactors, etc.). This includes a wide variety of processes in which convection and/or diffusion phenomenons are the leading ones. Among these, cite pressure-swing adsorption, tubular reactors arranged in series with a recycle, tubular reactors submitted to a periodic feed, electrochemical reactors with segmented electrodes.

2.1. Definition of the class of system under consideration

Consider a nonlinear system given by

$$\dot{x}(t) = A(u(t_{k-1}))x(t) + B(u(t_{k-1}))w(t) + \phi(x(t), u(t_{k-1}), w(t)); \quad t \in]t_{k-1}, t_k] \tag{2}$$

$$x(t_k^+) = Mx(t_k) \tag{3}$$

$$y(t) = H(u(t_{k-1}))x(t) \tag{4}$$

where

- $x \in \mathbb{R}^n$ is the state of the system; y is the measured output; u is a piece-wise constant control input while w is a measured exogenous signal.
- $(t_k)_{k\geqslant 0}$ is a strictly increasing sequence of switching instants w.r.t. which the piece-wise constant control u is defined.
- $x(t_k^+)$ stands for the state "*just after*" instant t_k in order for (3) to define a jump on the state arising at instant t_k.

The control input u and the measured exogenous signal w are assumed to belong to two compact sets, respectively, denoted by $\mathscr{U}$ and $\mathscr{W}$. Namely:

$$\forall t \in \mathbb{R}_+; \quad (u(t), w(t)) \in \mathscr{U} \times \mathscr{W} \tag{5}$$

furthermore, the following assumptions are needed:

Assumption 1. The nonlinear term in (2) is globally Lipschitz as a function of x uniformly in u and w. More precisely, there is a constant $K_\phi > 0$ such that

$$\forall (u, w) \in \mathscr{U} \times \mathscr{W};$$
$$\|\phi(x_1, u, w) - \phi(x_2, u, w)\| \leqslant K_\phi \cdot \|x_1 - x_2\| \tag{6}$$

Assumption 2. There exists a positive real $\tau_{\min}$ such that

$$\forall k, \quad t_{k+1} - t_k \geqslant \tau_{\min} \tag{7}$$

Assumption 3. For all $u \in \mathscr{U}$, the pair $(A(u), H(u))$ is observable. Moreover, there exists a positive real $\mu > 0$ such that for all $u \in \mathscr{U}$, there exists a positive definite matrix $Q(u)$ and a matrix gain $L(u)$ such that the following conditions hold:

(1) for all $u \in \mathscr{U}$:

$$-\lambda_{\min}(Q(u)) + 2K_\phi \|P(u)\| \leqslant -\mu \tag{8}$$

where $P(u)$ is the solution of the Lyapunov equation:

$$[A(u) - L(u)H(u)]^{\mathrm{T}} P(u) + P(u)[A(u) - L(u)H(u)] = -Q(u) \tag{9}$$

(2) for all $u \in \mathscr{U}$ there exists a positive $\gamma > 0$ such that

$$\mathscr{C}(\mathscr{U}) \cdot \lambda_{\max}^2(M) \cdot \mathrm{e}^{-\mu\tau_{\min}/\lambda_{\max}(P(u))} \leqslant \gamma < 1 \tag{10}$$

where $\mathscr{C}(\mathscr{U})$ is the positive real defined by

$$\mathscr{C}(\mathscr{U}) := \sup_{(u_1,u_2)\in\mathscr{U}\times\mathscr{U}} \left[\frac{\lambda_{\max}(P(u_1))}{\lambda_{\min}(P(u_2))}\right] \tag{11}$$

(3) There is a positive definite matrix $P_0 > 0$ such that

$$\forall u \in \mathscr{U}, \quad P(u) \geqslant P_0 > 0 \tag{12}$$

Remark 1. Let us explain why the conditions invoked in Assumption 3 are needed. Condition (8) guarantees that the decreasing term of the estimation error related Lyapunov function implied by the observer correction term overcomes the increasing term that may be caused by the nonlinear term in the system model. Condition (10) states that the duration between two jumps is sufficiently large to have a sufficient decrease in the Lyapunov function that overcomes the increase that may be induced by the state jump. Finally, condition (12) guarantees that all the above argumentation is still valid over the whole range of possible values of the control variable u.

2.2. Observer's definition

In order to estimate the state of the dynamical system (2)–(4), the following observer is used

$$\dot{\hat{x}}(t) = A(u(t_{k-1}))\hat{x}(t) + B(u(t_{k-1}))w(t) + \phi(\hat{x}(t), u(t_{k-1}), w(t)) + L(u(t_{k-1}))[y(t) - H(u(t_{k-1}))\hat{x}(t)] \tag{13}$$

$$\hat{x}(t_k^+) = M\hat{x}(t_k) \tag{14}$$

The following proposition can then be proved:

Proposition 1. *Under Assumptions* 1–3, *the dynamic system* (13) *and* (14) *is an asymptotic dynamic observer for the switched nonlinear system* (2)–(4).

Proof. See Appendix A. □

It goes without saying that Proposition 1 gives the theoretic framework under which the estimation scheme converges. Moreover, it is worth noting that all the inequalities used above are rather pessimistic since they result from worst-case based computation as it can be seen from the proof.

3. Application to the SMB

In this section, the equations of the SMB are recalled. The particular discretization procedure used in the derivation of the finite dimensional model is briefly commented. Finally, the way they can be put in the standard form (2)–(4) of Section 2 is shown.

3.1. Model

The SMB has been modelled by the following partial differential equations [11] representing, respectively, the mass balance for component i and the mass transfer from the liquid phase to the solid phase

$$\begin{aligned}&\frac{\partial c_i}{\partial t}+\frac{1-\epsilon}{\epsilon}\frac{\partial q_i}{\partial t}-D_{\mathrm{ax}}\frac{\partial^2 c_i}{\partial x^2}+v\frac{\partial c_i}{\partial x}=0\\&\frac{\partial q_i}{\partial t}=k_{\mathrm{eff},i}\frac{3}{R_p}(c-c_i^{\mathrm{eq}})\end{aligned}\tag{15}$$

where c_i and q_i are, respectively, the concentrations in the liquid and solid phase, ϵ is the porosity, D_{ax} is the apparent dispersion coefficient, v the fluid velocity in given section, R_{p} the adsorbent particle radius, $k_{\mathrm{eff},i}$ the mass transfer coefficient, c_i^{eq} the equilibrium concentration. The binary system is described by a competitive Langmuir nonlinear isotherm

$$q_i=\frac{N_iK_ic_i}{1+\sum_{j=1}^{n_{\mathrm{c}}}K_jc_j}\tag{16}$$

with N_i the saturation loading capacity of component i and K_i the Langmuir equilibrium constant. The values of the parameters used in the simulation are given in Table 1.

Table 1
Values of the parameters for SMB simulation

System parameters			
D	5 cm	L	50 cm
ϵ	0.4	D_{ax}	3×10^{-2} cm^2/s
K_{A}	1500 cm^3/g	K_{B}	2000 cm^3/g
N_{A}	5	N_{B}	5
$k_{\mathrm{eff,A}}$	3×10^{-4} cm/s	$k_{\mathrm{eff,A}}$	2.5×10^{-4} cm/s
Operating parameters			
Feed concentration $c_{\mathrm{f},i}$			5×10^{-4} g/cm^3
Feed flow rate Q_{f}			5.62 cm^3/s
Desorbent flow rate Q_{D}			100.644 cm^3/s
Extract flow rate Q_{E}			75.14 cm^3/s
Recycle flow rate Q_{IV}			103.56 cm^3/s
Switching period t_{switch}			30 s

3.2. Obtaining the canonical form (2)–(4)

After noticing that the mass transfer equation can be neglected with very little error, the resulting partial differential equation is

$$\frac{\partial c_i}{\partial t}+\frac{1-\epsilon}{\epsilon}\frac{\partial q_i}{\partial t}-D_{\mathrm{ax}}\frac{\partial^2 c_i}{\partial x^2}+v\frac{\partial c_i}{\partial x}=0\tag{17}$$

where c_i and q_i are related by the equilibrium equation such that $q_i=q_i(c_{\mathrm{A}},c_{\mathrm{B}})$. First, this equation is spatially discretized by means of finite differences. The resulting ordinary differential system is of the form

$$E(c)\dot{c}=F(u)c+G(u)c_{\mathrm{f}}\tag{18}$$

where c_{f} is the feed concentration vector $[c_{\mathrm{Af}},c_{\mathrm{Bf}}]^{\mathrm{T}}$ which is a measured exogenous signal. m_{t} being the total number of discretization elements in the SMB, the chemical system being binary, the vector c has dimension $2m_{\mathrm{t}}$ and is formed by the successive vectors $[c_{\mathrm{A}}^j,c_{\mathrm{B}}^j]$ where j is the index of a spatial element, starting from the first element of Section 1, ending at the last element of Section 4. $F(u)$ and $G(u)$ depend on the flow rates and thus on the manipulated input vector u equal to $[Q_{\mathrm{D}},Q_{\mathrm{IV}},Q_{\mathrm{E}},t_{\mathrm{switch}}]$. In the general case of a nonlinear equilibrium law, the matrix $E(c)$ is block diagonal with its subelements of dimension 2×2. If the equilibrium law is linear, $E(c)$ is strictly diagonal and constant. In any case, $E(c)$ can be easily inverted resulting in

$$\dot{c}=E^{-1}(c)F(u)c+E^{-1}(c)G(u)c_{\mathrm{f}}\tag{19}$$

Then, $E^{-1}(c)$ is decomposed into two contributions, one equal to $E^{-1}(c=0)$ and denoted by E_0^{-1}, the other one depending on c and is equal to $[E^{-1}(c)-E^{-1}(c=0)]$ and denoted by E_{c}^{-1}, so that the system becomes

$$\dot{c}=E_0^{-1}F(u)c+E_{\mathrm{c}}^{-1}F(u)c+E^{-1}(c)G(u)c_{\mathrm{f}}\tag{20}$$

with a linear term, a nonlinear term and a disturbance term.

The matrix M representing the shift operation is easily obtained from the representation of the vector c just before and after the shift

$$c^+=Mc^-\tag{21}$$

The measured outputs are the concentrations c_{A} and c_{B} at the different streams of the SMB, i.e. the extract, the inlet of Section 3, the raffinate and lastly the recycle or outlet of Section 4. Furthermore, the measurements are assumed to be instantaneous. From this definition of the outputs, the matrix H is deduced.

To summarize, the system can be put in the general form (2)–(4) with the following definitions (with $x=c$ and $w=c_{\mathrm{f}}$)

$$\begin{aligned}A(u)&=E_0^{-1}F(u);\quad \phi(x,u)=E_{\mathrm{c}}^{-1}F(u)c;\quad B(u)\\&=E_0^{-1}G(u)+E_{\mathrm{c}}^{-1}G(u)\end{aligned}\tag{22}$$

3.3. Some implementation issues

The convection term has been discretized according to a finite difference of order 1, while the diffusion term has been discretized according to a centered finite difference of order 2. Ten discretization points per column were chosen. The influence of the diffusion term was low compared to other parameters such as the equilibrium constants. The SMB contained two columns per section.

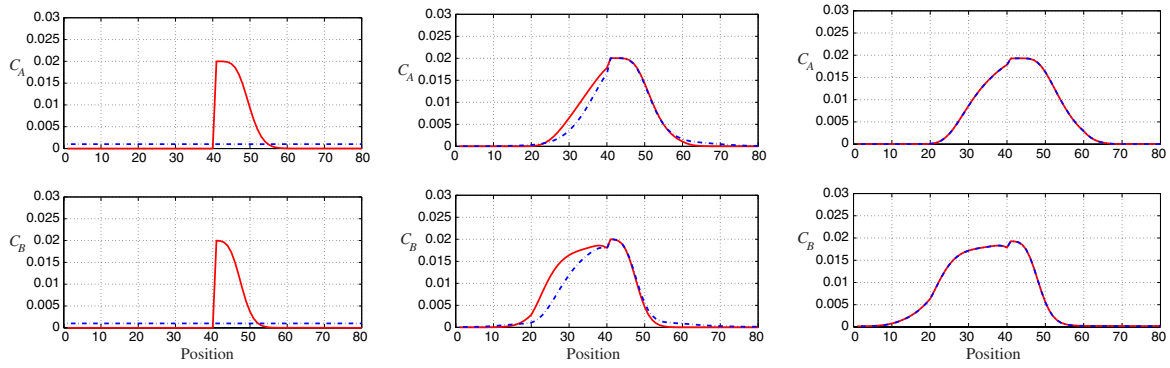

Fig. 2. Spatial profiles of component A (top) and B (bottom) in the SMB at the end of the 1st, 8th and the 30th switching periods. Continuous line (real states), dashed line (estimated states). (Conditions: no measurement noise, no model errors, *no correction term in the observer*.)

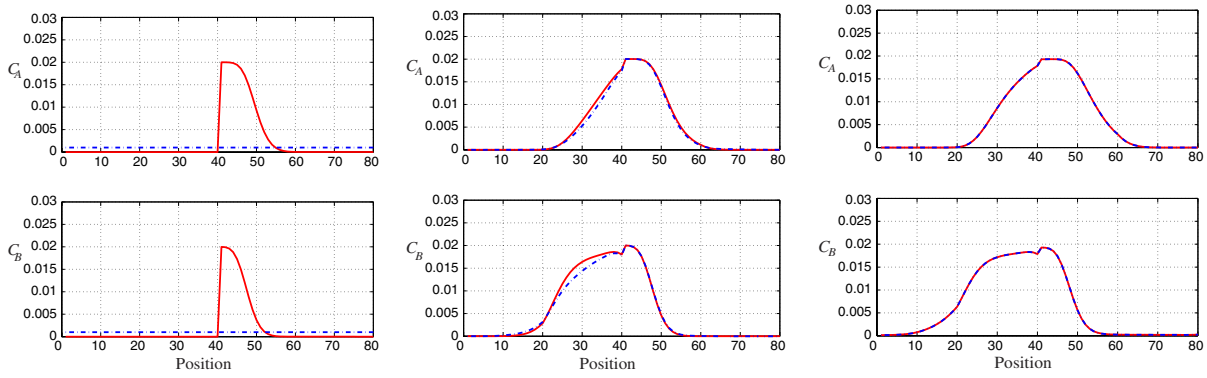

Fig. 3. Spatial profiles of component A (top) and B (bottom) in the SMB at the end of the 1st, 8th and the 30th switching periods. Continuous line (real states), dashed line (estimated states). (Conditions: no measurement noise, no model errors, *correction term in the observer*.)

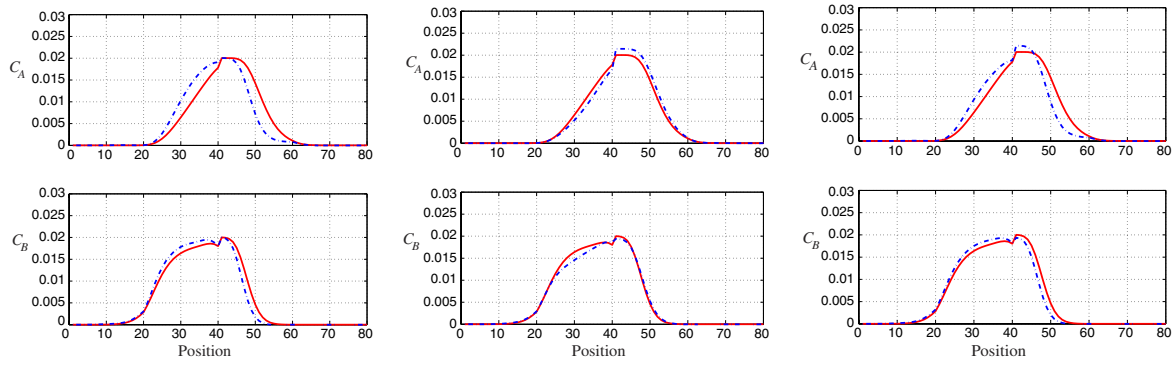

Fig. 4. Influence of various modelling errors on the spatial profiles of component A (top) and B (bottom) in the SMB at the end of the eighth switching period. Continuous line (real states), dashed line (estimated states). In all cases, measurement normal noise ($\sigma = 0.25$) and *correction term in the observer*. (Left conditions: model errors on the equilibrium constants K_i and N_i (5%), correction term in the observer.) (Middle conditions: model errors on the flow rates (±5%) and the feed concentration (±5%), correction term in the observer.) (Right conditions: model errors on the equilibrium constants K_i and N_i (5%), the flow rates (±5%) and the feed concentration (±5%).)

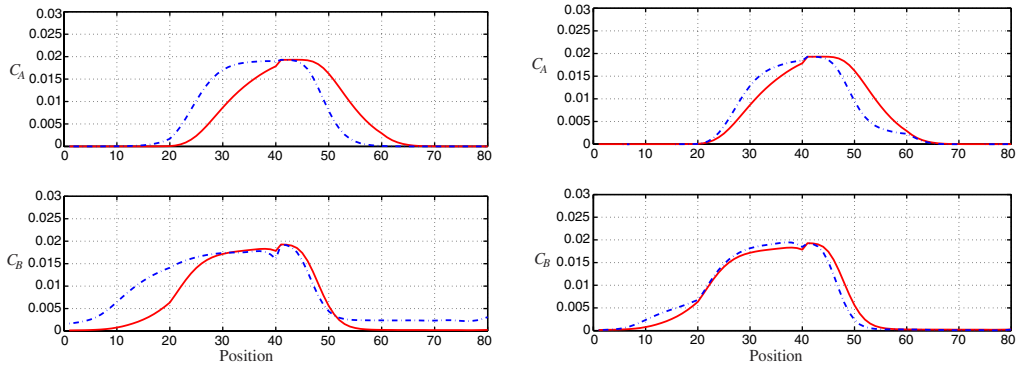

Fig. 5. Influence of the correction term of the observer on the spatial profiles of component A (top) and B (bottom) in the SMB at the end of the 30th switching period. Continuous line (real states), dashed line (estimated states). In both cases, measurement normal noise ($\sigma = 0.25$), model errors on the equilibrium constants K_i and N_i (5%). (Left conditions: *no correction term in the observer*.) (Right conditions: *correction term in the observer*.)

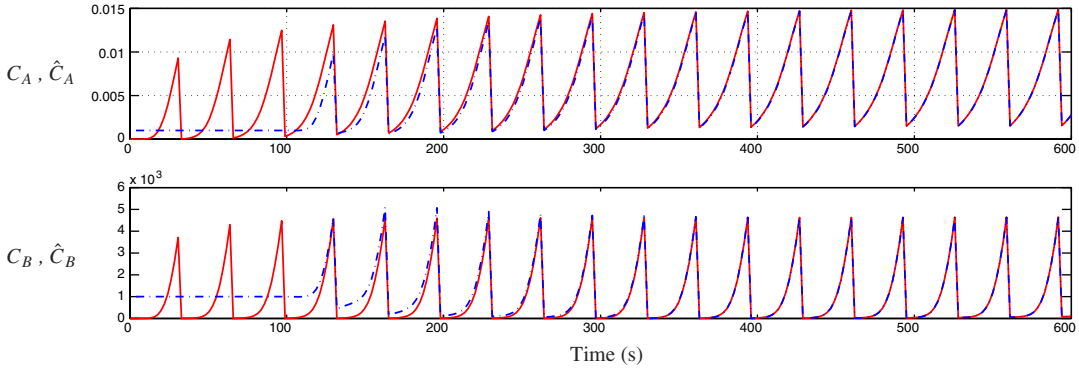

Fig. 6. Convergence of the observer for a point located at middle of Section 3 of the SMB for components A (top) and B (bottom). Continuous line (real states), dashed line (estimated states). (Conditions: no measurement noise, no model errors, *correction term included in the observer*.)

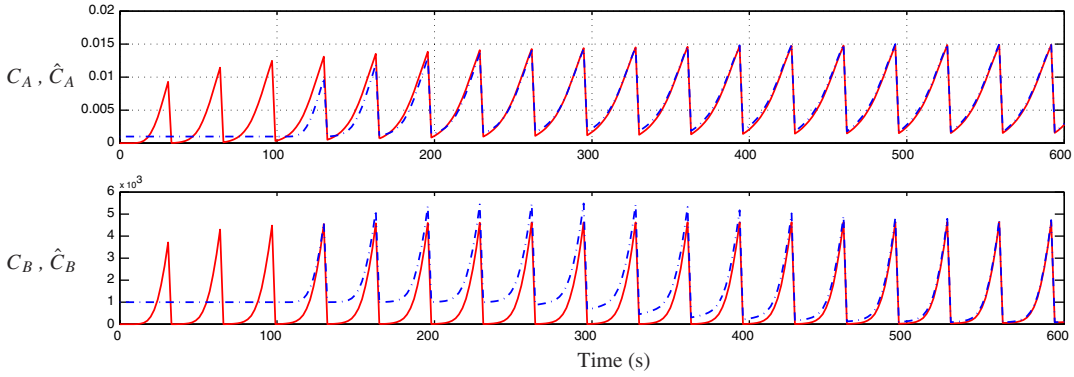

Fig. 7. Behavior of the free-correction observer for a point located at middle of Section 3 of the SMB for components A (top) and B (bottom). Continuous line (real states), dashed line (estimated states). (Conditions: no measurement noise, no model errors, *no correction term included in the observer*.)

Different sets of data taken from various papers have been used to test the behaviour of the observer. In our set, the switching time is low compared to most references, which is not an advantage, however the data are self-consistent.

The computation of the observer gain $L(u)$ that is used in the observer Eqs. (13) has been done using the dual linear quadratic regulator design[1] with some suitably chosen weighting matrices $Q_{\mathrm{Reg}} \in \mathbb{R}^{160\times160}$ and $R_{\mathrm{Reg}} \in \mathbb{R}^{8\times8}$. This enables to find $L(u)$ such that the Lyapunov Eq. (9) is satisfied with Q given by

[1] This has been done using the Matlab's subroutine LQR in which the matrices $A^{\mathrm{T}}(u)$, H^{T}, Q_{Reg} and R_{Reg} have been used.

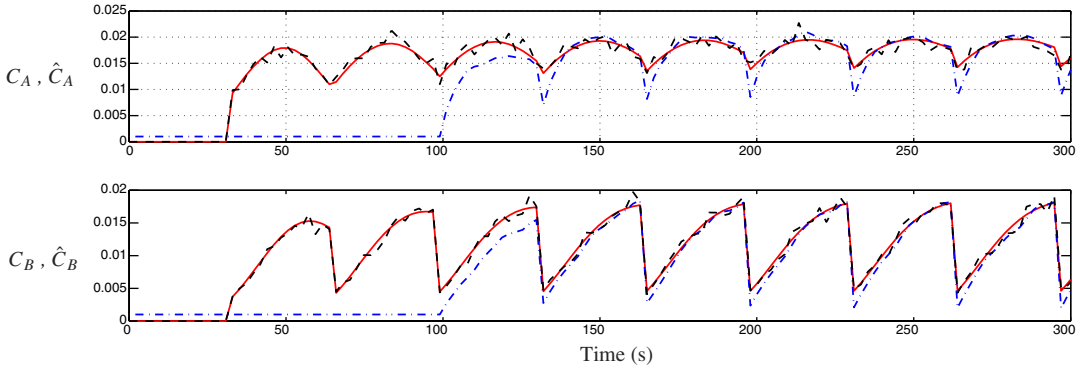

Fig. 8. Convergence of the observer for the feed point of the SMB for components A (top) and B (bottom). Continuous line (real states), dashed-point line (estimated states), dashed line (measurements). (Conditions: measurement normal noise ($\sigma = 0.25$), model errors on the equilibrium constants K_i and N_i (5%), the flow rates (±5%) and the feed concentration (±5%), *correction term included in the observer*.)

$$Q(u) = Q_{\text{Reg}} + L(u)R_{\text{Reg}}L(u)^{\text{T}}$$

This is possible if the pair ($A(u)$, H) is observable which has been tested for some hyper-cube centered on some nominal value of the flow rates corresponding to good separation regime. It is worth noting that in a realistic context, the choice of the matrices Q_{Reg} and R_{Reg} has to be done based on the statistical characterizations of the measurement noise (covariance matrices).

4. Simulation results

The simulations have been first performed with the model taking into account the mass transfer equation. It was found that when no mass transfer resistance was considered, so that the equilibrium between liquid and solid phases was assumed, the difference was not noticeable. Consequently, the simplified model with Langmuir nonlinear equilibrium was considered in the following. However, the real states are obtained by a more rigorous model than the states of the observer.

In all cases, initially the states of the process are equal to zero. At time zero, the model of the process starts but the observer starts only after three switching periods and starts with nonzero initial estimated states.

Different scenario have been successively tested to check the influence of various model errors and of measurement noises following the normal law, as well as the influence of the correction term in the observer. The chosen times were the end of the first switch corresponding to a time close to initialization, the end of the eighth switch to an intermediate time, the end of the 30th switch to a time when normally the stationary regime is established.

The spatial profiles of real and estimated components show that in absence of correction term in the observer (Fig. 2), even in absence of any noise or modelling errors, the convergence towards the real state is slower (compare to Fig. 3). The model errors have various influences on the estimated spatial profile. In Fig. 4, it appears that the errors on the equilibrium coefficients influence the estimated states more than the errors on the flow rates or on the feed concentration. However, in spite of relatively large errors on all these parameters, the states are correctly estimated. The influence of the correction term of the observer is clearly demonstrated in Fig. 5. In the absence of this correction term, after 30 switches, the deviation between the real and the estimated profiles is considerable and the presence of this correction term is necessary.

The convergence has been shown for a point of a wave front located at mid-distance between two measurements in the third section. In the absence of model errors, the observer with correction term converges in approximately three switching periods towards the real state (Fig. 6) while the free-correction term simulation based observer converges much more slowly since about 10 switching periods are necessary for the estimated profiles to converge to the real ones (Fig. 7).

Finally Fig. 8 enables to appreciate the noise level by showing the behavior of the feed point measurements and the corresponding estimation under several modelling errors.

5. Conclusion and future work

In this paper, a systematic approach is proposed for the design of a state observer for a class of nonlinear switched systems. Application to SMB with nonlinear isotherm under parameter uncertainties show good performance and robustness properties. However, simulations under uncertainties underline the high sensitivity of the estimation errors to errors on the isotherm coefficients (K_i and N_i). This suggests that the proposed observer must be coupled with a parametric estimation module that feeds it with corrected values of the key isotherm parameters mentioned above. The fact that steady

state regimes are independent of initial state makes this reasonably achievable.

Acknowledgement

This research has been funded by a French government program entitled "*ACI-Nouvelle Methodologies analytiques et capteur*".

Appendix A. Proof of proposition

Using e to denote the estimation error, namely

$$e(t) = x(t) - \hat{x}(t) \tag{23}$$

direct computation leads to the following error dynamics

$$\dot{e}(t) = [A(u(t_{k-1})) - L(u(t_{k-1}))H(u(t_{k-1}))]e(t) + \phi(x(t), u(t_{k-1}), w(t)) - \phi(\hat{x}(t), u(t_{k-1}), w(t)) \tag{24}$$

$$e(t_k^+) = Me(t_k) \tag{25}$$

Using the notation

$$V(e,u) = e^{\mathrm{T}}P(u)e$$

one can write for all $t \in [t_{k-1}^+, t_k[$ using (9)

$$\dot{V}(e(t), u(t_{k-1})) \leqslant [-\lambda_{\min}(Q(u(t_{k-1}))) + 2K_\phi \cdot \|P(u(t_{k-1}))\|]\|e(t)\|^2 \tag{26}$$

hence, by virtue of (8), it comes that for all $t \in [t_{k-1}^+, t_k]$

$$\dot{V}(e(t), u(t_{k-1})) \leqslant -\frac{\mu}{\lambda_{\max}(P(u(t_{k-1})))} V(e(t), u(t_{k-1}))$$

therefore

$$V(e(t_k, u(t_{k-1}))) \leqslant e^{-\mu\tau_{\min}/\lambda_{\max}(P(u(t_{k-1})))} \cdot V(e(t_{k-1}^+, u(t_{k-1}))) \tag{27}$$

Let us now compute $V(e(t_k^+), u(t_k))$. By definition, one has

$$\begin{aligned} V(e(t_k^+), u(t_k)) &:= e^{\mathrm{T}}(t_k)M^{\mathrm{T}}P(u(t_k))Me(t_k) \\ &\leqslant \lambda_{\max}^2(M)\lambda_{\max}(P(u(t_k)))\|e(t_k)\|^2 \\ &\leqslant \lambda_{\max}^2(M)\lambda_{\max}(P(u(t_k))) \\ &\quad \times \frac{1}{\lambda_{\min}(P(u(t_{k-1})))} V(e(t_k), u(t_{k-1})) \end{aligned}$$

and using (27), one obtains

$$V(e(t_k^+), u(t_k)) \leqslant \lambda_{\max}^2(M)\mathscr{C}(\mathscr{U}) \cdot e^{-\mu\tau_{\min}/\lambda_{\max}(P(u(t_{k-1})))} \cdot V(e(t_{k-1}^+, u(t_{k-1}))) \tag{28}$$

which, by virtue of (10) gives

$$V(e(t_k^+), u(t_k)) \leqslant \gamma \cdot V(e(t_{k-1}^+, u(t_{k-1})))$$

therefore, according to assumption (12)

$$\lim_{k\to\infty} e^{\mathrm{T}}(t_k^+)P_0e(t_k^+) \leqslant \lim_{k\to\infty} V(e(t_k^+), u(t_k)) = 0 \tag{29}$$

and since P_0 is positive definite, it comes that

$$\lim_{k\to\infty} e(t_k^+) = 0$$

This together with the consistency if the observer equation and the continuity of the jump map clearly prove the result.

The output matrix H concerns the measured states which are both components in the extract, feed, raffinate and recycle streams. The components of the state vector c start from the first element of discretization in Section 1 and end at the last element of discretization in Section 4. Assume that there are m elements of discretization in each section ($m = 2n_c$) and two components. The matrix H is a matrix of dimension $(8 \times n)$ with $n = 8m$ and with all elements equal to 0 except $H(1, 2m-1) = 1$, $H(2, 2m) = 1$, $H(3, 4m-1) = 1$, $H(4, 4m) = 1$, $H(5, 6m-1) = 1$, $H(5, 6m) = 1$, $H(7, 8m-1) = 1$, $H(8, 8m) = 1$.

The commutation matrix M can be decomposed as

$$M = \begin{bmatrix} M_{11} & I_{12} \\ I_{21} & M_{22} \end{bmatrix} \tag{30}$$

where M_{11} and M_{22} are null matrices, I_{21} and I_{12} are identity matrices. The size of I_{21} is equal to $4n_c$ (2 components $\times$ 2 columns per section $\times$ n_c elements of discretization per column). The size of I_{12} is equal to $12n_c$. Thus the total size of M corresponds to the discretization of eight columns.

References

[1] M. Alamir, J.P. Corriou, Nonlinear receding horizon state estimation for dispersive adsorption columns with nonlinear isotherm, J. Process Cont. 13 (6) (2003) 517–523.
[2] M. Alamir, F. Ibrahim, J. P. Corriou. A flexible nonlinear model predictive control scheme for quality/performance handling in nonlinear SMB chromatography, J. Process Cont., in press, doi:10.1016/j.jprocont.2005.07.001.
[3] D. Broughton, C. Gerhold. Continuous sorption process employing fixed bed of sorbent and moving inlets and outlets, US Patent 2985589, 1961.
[4] F. Charton, R.M. Nicoud, Complete design of a simulated moving bed, J. Chromatogr. A 702 (1995) 97–112.
[5] C.B. Ching, Analysis of the performance of a simulated countercurrent chromatographic system for fructose–glucose separation, Can. J. Chem. Eng. 62 (1984) 398–403.
[6] C.B. Ching, K.H. Chu, K. Hidajat, M.S. Uddin, Comparative study of flow schemes for a simulated counter-current adsorption separation process, AIChE J. 38 (11) (1992) 1744–1750.
[8] N. Couenne, G. Bornard, J. Chebassier, D. Humeau, Contrôle et optimisation d'une unité de séparation de xylènes par contre-courant simulé, in: SIMO 2002, Toulouse, France, 2002.
[9] G. Dünnebier, K.-U. Klatt, Modelling and simulation of nonlinear chromatographic separation processes: a comparison of different modelling approaches, Chem. Eng. Sci. 55 (2000) 373–380.

[10] G. Dünnebier, I. Weirich, K.-U. Klatt, Modeling fixed-bed adsorption columns through orthogonal collocations on moving finite elements, Comput. Chem. Eng. 21 (6) (1997) 641–660.
[11] G. Dünnebier, I. Weirich, K.-U. Klatt, Computationally efficient dynamic modelling and simulation of simulated moving bed chromatographic processes with linear isotherms, Chem. Eng. Sci. 53 (14) (1998) 2537–2546.
[12] G. Erdem, S. Abel, M. Morari, M. Mazotti, M. Morbidelli, J.H. Lee, Automatic control of simulated moving beds, Ind. Eng. Chem. Res. 43 (2004) 405–421.
[13] E.R. Francotte, P. Richert, Applications of simulated moving-bed chromatography to the separation of the enantiomers of chiral drugs, J. Chromatogr. A. 769 (1997) 101–107.
[14] J. Haag, A. Vande Wouver, S. Lehoucq, P. Saucez, Modeling and simulation of a smb chromatographic process designed for enantioseparation, Cont. Eng. Pract. 9 (2001) 921–928.
[15] K.-U. Klatt, F. Hanisch, G. Dünnebier, Model-based control of a simulated moving bed chromatographic process for the separa-tion of fructose and glucose, J. Process Cont. (12) (2002) 203–219.
[16] T. Kleinert, J. Lunze, Modelling and state observation of simulated moving bed processes, in ECC03: European Control Conference, Cambridge, UK, 2003.
[17] E. Kloppenburg, E.D. Gilles, Automatic control of the simulated moving bed process for C_8 aromatics separation using asymptotically exact input–output linearization, J. Process Cont. (1) (1999) 41–50.
[18] S. Lehoucq, S. Verhève, A. Vande Wouver, E. Cavoy, Smb enantio separation: process development modeling and operating conditions, AIChE J. 46 (2000) 247–256.
[19] Y. Lim, S.B. Jörgensen, Optimization of simulated moving bed (smb) chromatography: a multi-level optimization procedure, in: ESCAPE-14: European Symposium on Computer Aided Process Engineering, Lisbon, Portugal, 2004.
[20] O. Ludemann-Hombourger, R.M. Nicoud, The VARICOL process: a new multicolumn continuous chromatographic processes, Sep. Sci. Technol. 35 (12) (2000) 1829–1862.
[21] M. Mangold, G. Lauschke, J. Schaffner, M. Zeitz, E.D. Gilles, State and parameter estimation for adsorption columns by nonlinear distributed parameter state observers, J. Process Cont. 4 (3) (1994) 163–171.
[22] M. Mazzotti, G. Storti, M. Morbidelli, Robust design of countercurrent adsorption separation: 3. Nonstoichiometric system, AIChE J. 42 (1996) 2784–2796.
[23] M. Mazzotti, G. Storti, M. Morbidelli, Optimal operation of simulated moving bed units for nonlinear chromatographic separations, J. Chromatogr. A. 769 (1997) 3–24.
[24] S. Natarajan, J.H. Lee, Repetitive model predictive control applied to a simulated moving bed chromatography system, Comput. Chem. Eng. 24 (2000) 1127–1133.
[25] R.M. Nicoud, The simulated moving bed: a powerful chromatographic process, LC–GC Int. 5 (1992) 43–47.
[26] D.E. Rearick, M. Kearney, D.D. Costesso, Simulated moving-bed technology in the sweetener industry, Chemtech 27 (1997) 36–40.
[27] D. Ruthven, C.B. Ching, Counter-current and simulated counter-current adsorption separation processes, Chem. Eng. Sci. (5) (1989) 1011–1038.
[28] G. Storti, M. Masi, S. Carra, M. Morbidelli, Modelling and design of simulated moving bed units, Prep. Chromatogr. 1 (1) (1988) 1–27.
[29] M. Ben Thabet, M. Alamir, M. Bailly, J.P. Corriou, Nonlinear control of a simulated moving bed, in: Conference on Separation Science and Technologies, AIChE 97, Los Angeles, pp. 1316–1321, 1997.
[30] G. Zimmer, G. Dünnebier, K.U. Klatt, On-line parameter estimation and process monitoring of simulated moving bed chromatographic processes, in: European Control Conference ECC 99, 1999.